ELSEVIER

Biochimica et Biophysica Acta 1318 (1997) 374–384

BIOCHIMICA ET BIOPHYSICA ACTA
BBA

Photo-induced cyclic electron transfer operates in frozen cells of *Rhodobacter sphaeroides*

Pierre Joliot [a,*], Anne Joliot [a], André Verméglio [b]

[a] *CNRS (UPR 9072) Institut de Biologie Physico-Chimique, 13, rue Pierre-et-Marie-Curie, 75005 Paris, France*
[b] *DEVM / LBC, CEA Cadarache, 13108 Saint-Paul-lez-Durance Cedex, France*

Received 16 April 1996; accepted 11 September 1996

Abstract

The three phases of the flash-induced membrane potential rise were measured in *Rhodobacter sphaeroides*, at temperatures between 16°C and −30°C, in the liquid or the frozen state. We show that phase II, which is myxothiazol-insensitive, includes phase IIa and phase IIb, completed at −8°C in about 2 ms and 10 ms, respectively. Phase IIa is very likely associated with the protonation of the doubly-reduced quinone acceptor $Q_B^{=}$ (Drachev, L.A., Mamedov, A., Mulkidjanian, A.Y., Semenov, A.Y., Shinkarev, V.P. and Verkhovsky, M.J. (1988) FEBS Lett. 233, 315–318); phase IIb is associated with the oxidation of cytochrome c_2 (Jackson, J.B. and Dutton, P.L., 1973, Biochim. Biophys. Acta 325, 102–113). Freezing the sample does not modify the kinetics of phase IIa but slows down phase IIb by a factor of 2. The amplitude of phase III, which is exclusively related to electron and proton transfer within the cytochrome b/c_1 complex, is temperature-independent between room temperature and −16°C. In the frozen state, the rate of phase III is mainly limited by the electron transfer from cytochrome c_2 to the reaction centers and not by the movement of cytochrome c_2 between the two membrane complexes. These results are interpreted assuming that one cytochrome c_2 is trapped in a supercomplex formed by the association of two reaction centers and one cytochrome b/c_1 complex.

Keywords: Membrane potential; Cytochrome bc_1 complex; Cytochrome c_2; Supercomplex; Electron transfer; Low-temperature spectroscopy; (*Rhodobacter sphaeroides*)

1. Introduction

In several papers [1–3], we have investigated the structural organization of the photosynthetic electron transfer chain in *Rhodobacter* (*Rb.*) *sphaeroides*. Thermodynamic and kinetics analyses of electron transfer reactions led us to conclude that in this species, most of the photosynthetic electron transfer chains are organized in supercomplexes including two reaction centers (RC), one cytochrome (cyt) b/c_1 complex and one cyt c_2 [1,3,4]. In this model, thermodynamic equilibration among primary and secondary donors within a supercomplex is completed in about 1 ms, while equilibration between supercomplexes is a much slower process. This implies that one cyt c_2 molecule, trapped within the supercomplex, is not able to freely diffuse in the aqueous phase. In *Rb. sphaeroides* (Ga strain), we reported that the electron transfer chains are organized in supercomplexes only in the chromatophore compart-

Abbreviations: Cyt, cytochrome; DMSO, dimethylsulfoxide; P, primary donor P_{870}; RC, reaction center; *Rb*, *Rhodobacter*; *Rs*, *Rhodospirillum*.

* Corresponding author. Fax: +33 1 40468331. E-mail: ajoliot@ibpc.fr

PII S0005-2728(96)00114-4

ment. Cyt c_2 is able to diffuse in the periplasmic compartment, where both respiratory and photosynthetic chains are included [3].

Measurements of the light-induced formation of the membrane potential is a powerful tool to analyse the transmembrane electron and proton movements occurring at the level of the two complexes of the photosynthetic chain. Following a short-flash excitation, the membrane potential increase displays three phases [5,6] and is reviewed in Ref. [7]. Phase I (<1 ns) is associated with the charge separation between the primary donor P_{870} (P) and the primary quinone acceptor Q_A. Phase II is completed in about 1 ms at room temperature and its amplitude is 20–30% of phase I. Phase II was first ascribed to an electrogenic step associated with the electron transfer from cyt c_2 to P^+ [5,6]. Kaminskaya et al. [8] and Drachev et al. [9] proposed that phase II is associated with both the reduction of P^+ by cyt c_2 and the proton binding to the doubly reduced acceptor $Q_B^=$. Phase III, completed in 10 ms in reducing conditions, has an amplitude comparable to that of phase I. It is inhibited by myxothiazol [10] and is associated with electron transfer processes occurring within the cyt b/c_1 complex.

Freezing the sample is a simple way to modify the rate of diffusion of mobile carriers. Using *Rs. rubrum* and *Rb. sphaeroides* cells suspended in a 'non-crystallizing medium', with antifreeze, Vredenberg and Duysens [11] observed a photooxidation of cytochrome under continuous illumination at -30°C. In this paper, we investigated the flash induced electron transfer between primary and secondary donors and the membrane potential rise as a function of temperature in the liquid and frozen states. Freezing the sample in the absence of high concentration of antifreeze will specifically affect electron transfer reactions involving long-range diffusion of soluble components and will provide new insight on the supramolecular organization of the photosynthetic electron transfer chain.

2. Materials and methods

2.1. Material

Rb. sphaeroides were grown at 30°C in Hutner medium. The bacteria were exposed to white light, provided by incandescent bulbs. When stated, the cells were treated for 1 min with 100 μM benzoquinone. Bacteria were centrifuged and resuspended in 50 mM phosphate buffer (pH 7.2) in order to eliminate benzoquinone in excess. The benzoquinone treatment inhibits the respiration by slowing down the input of electrons with no modification in the activity of the terminal oxidase. Benzoquinone treatment also inhibits the membrane ATP-synthase [12] and thus collapses the permanent membrane potential observed in living cells, which arises from the hydrolysis of intracellular ATP and from respiration. The redox state of the ubiquinone pool (as estimated from the half-time of phase III) was adjusted by varying the KCN concentration and the incubation time of the sample at room temperature in the measuring cuvette. Low temperature experiments were performed in the presence of 5% (v/v) dimethylsulfoxide (i.e., 60 mM DMSO) which acts as a cryoprotector. At room temperature, we do not observe any effect of the addition of DMSO on the kinetics of electron transfer or on the membrane potential rise.

2.2. A new spectrophotometric method adapted to sub-zero-temperature measurements

A highly sensitive spectrophotometric method has been developed by D. Béal and P. Joliot, adapted to measurements of light-induced spectral changes in biological samples at temperatures between 30°C and -50°C. As described in Refs. [13,14], the absorption level is sampled using 2-μs monochromatic flashes given at various intervals after the actinic excitation. To adapt this technique to low-temperature measurements, the biological material is placed in measuring and reference cuvettes 0.2 mm thick (1.35 cm^2 surface). The rear face of each cuvette is formed by a 1-mm thick polished aluminum plate which reflects actinic and detecting light. The temperature of the sample can be adjusted to values between 35°C and -40°C, using a Peltier device Melcor CP-2-15-10L, which is glued on the rear face of the aluminum plate. Two temperatures can be preset, allowing a rapid switch of temperatures (less than 1 min).

An unexpected behavior is that the sample can be renewed at sub-zero temperatures, showing that it remains in a supercooled state during several minutes, even in the absence of antifreeze. The tempera-

ture of freezing, which occurs around −11°C, does not depend upon the presence of biological material, buffer or salts. As expected, thawing of the sample always occurs at 0°C. It is then possible, in the temperature range 0°C to −11°C, to perform kinetics analyses of electron transfer reactions at the same temperature, either in a liquid or in a frozen state. The addition of 5% (v/v) DMSO does not significantly modify the freezing or thawing temperatures of the suspension.

The freezing of the suspension induces a small absorption increase due to the formation of ice. Within the 0.2-mm thick cuvette, the ice layer remains translucid. We observed that freezing the sample did not markedly modify the amplitude of the light-induced absorption changes.

The amplitude of the carotenoid shift, which is proportional to the membrane potential, was measured as the difference $\Delta I/I$ (503 nm–490 nm). The redox changes of the primary donor P were measured at 542 nm, an isobestic point for cyt c_t (cyt c_1 + cyt c_2) spectral changes.

3. Results

3.1. Membrane potential decay

The kinetics of the membrane potential decay were studied in whole cells after a benzoquinone-treatment which blocks the membrane ATP-synthase [12]. In these conditions, and at a temperature above −16°C, the membrane potential decay is mainly associated with transmembrane ion leaks. The decay of the membrane potential is temperature-dependent with half-times of ≈3 s at 16°C and ≈30 s at −16°C (not shown). In Fig. 1, the logarithm of the rate of the membrane potential decay, measured after completion of the increasing phases (phase I, II and III), is plotted as a function of the reciprocal of the absolute temperature. This Arrhenius plot displays two linear ranges corresponding to an activation enthalpy of 40 kJ mol^{-1} in the liquid state and 60 kJ mol^{-1} in the frozen state between −8°C and −16°C. Below −16°C, the rate of the back reactions between P^+ and the reduced quinone acceptors becomes significant compared with the rate of ion leaks (see below), which explains the non-linearity of the Arrhenius plot

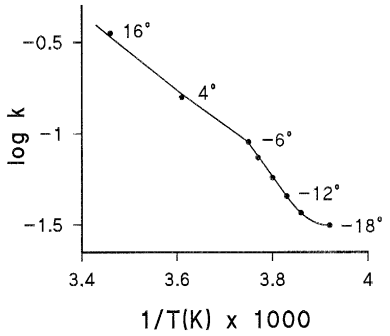

Fig. 1. Temperature-dependence of the rate constant of the membrane potential decay (Arrhenius plot). Benzoquinone-treated cells. The cells were incubated for 15 min in the presence of 2 mM KCN at 16°C.

in this temperature range. In the absence of DMSO, freezing the suspension induces a drastic acceleration of the membrane potential decay ($t_{1/2} < 10$ ms), very likely due to the formation of large ice crystals which destroy the membrane integrity. Addition of 5% (v/v) DMSO very likely decreases the size of the ice crystals; this would explain the action of DMSO as a cryoprotector at such a low concentration.

Fig. 2 shows the membrane potential decay and P^+ reduction measured with whole cells at −32°C under different redox conditions. Reducing conditions

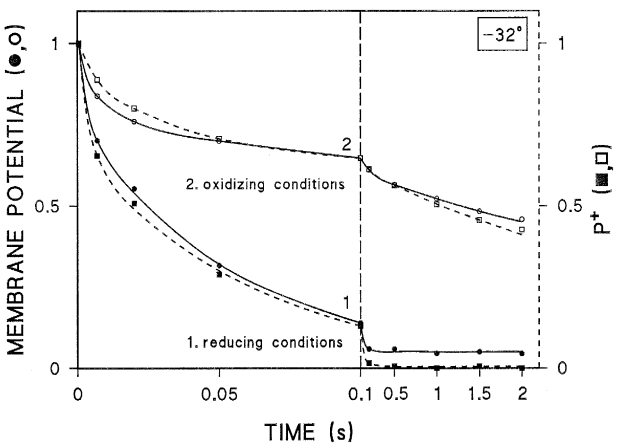

Fig. 2. Flash-induced membrane potential changes and P^+ reduction at −32°C. (1) Reducing conditions (closed symbols). Untreated cells. 4 mM KCN. Saturating-flash excitation 2 min apart. (2) Oxidizing conditions (open symbols). Benzoquinone-treated cells. 2 mM KCN. The sample was frozen immediatly after filling the cuvette. Non-saturating flash excitation, hitting ≈50% of the RCs. The membrane potential is normalized to the amplitude of phase I.

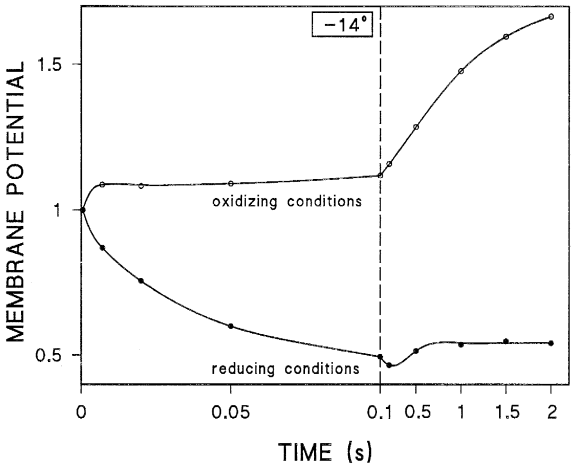

Fig. 3. Flash-induced membrane potential changes at −14°C. Same sample and same conditions as in Fig. 2.

(curves 1) were obtained using untreated cells incubated 15 min at room temperature, in the presence of 4 mM KCN. The redox state of Q_A was estimated by measuring the amplitude of phase I, which is proportional to the number of primary charge separations. Under these conditions, ≈ 50% of Q_A is reduced. On the basis of the mid-point potential of Q_A (≈ −50 mV at pH 7) and that of the ubiquinone pool (+50 mV) and taking into account that ubiquinone is a two-electron carrier, one expects that, under these conditions, the pool of ubiquinone and the secondary quinone acceptor Q_B are less than 0.1% oxidized. Then, following a flash, P^+ reduction and the membrane potential decay are associated with the back reaction between P^+ and Q_A^- ($t_{1/2} \approx 23$ ms). Using benzoquinone-treated cells shortly incubated in the presence of KCN, Q_A is fully oxidized and a large fraction of the ubiquinone pool is in its oxidized form. Curves 2 were obtained using non-saturating flashes which hit ≈ 50% of RCs in order to induce about the same number of charge separations as in curves 1. In these oxidizing conditions, most of P^+ reduction and of the decay of membrane potential occur in a range of several seconds ($t_{1/2} \approx 3$ s). A fast phase (≈ 25% of the amplitude) is completed in ≈ 200 ms. It is worth noting that, irrespective of the redox conditions, the kinetics of the membrane potential decay are close to those of P^+ reduction at −32°C. This shows that, at this temperature, both processes are controlled by back reactions between P^+ and the reduced quinone acceptors.

In Fig. 3, the membrane potential changes were measured at −14°C, under the same conditions and using the same sample as in Fig. 2. In oxidizing conditions, a fast increasing phase, corresponding to ≈ 9% of phase I, is followed by a slow increase mainly associated with phase III. In reducing conditions, the membrane potential decays during the first hundred ms. Then, a slow increasing phase is observed in the 1-s time-range.

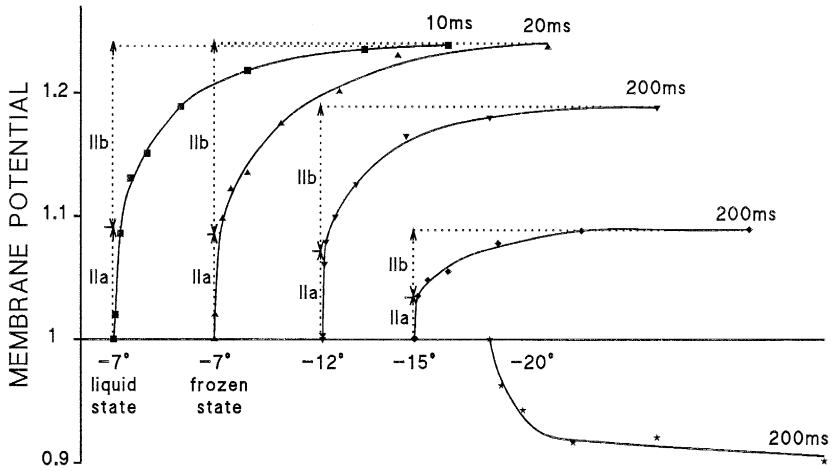

Fig. 4. Kinetics of phase II as a function of temperature. Benzoquinone-treated cells. 20 μM myxothiazol. 1 mM KCN. 10 min incubation at room temperature. Saturating-flash excitation 1 min apart in the liquid state and 2 min apart in the frozen state. The membrane potential is normalized to the amplitude of phase I. IIa: phase IIa. IIb: phase IIb. Below −7°C, all samples were in the frozen state.

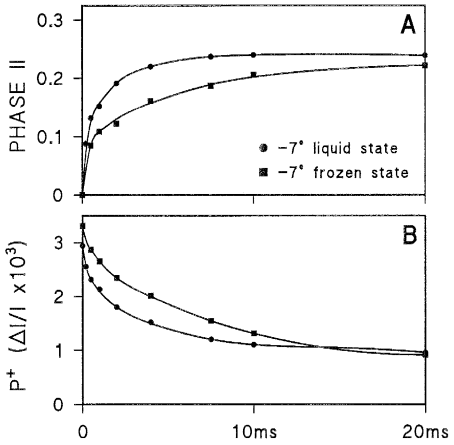

Fig. 5. Kinetics of phase II and P^+ reduction at -7°C in the liquid or the frozen state. Same conditions as in Fig. 4. The amplitude of phase II is normalized to the amplitude of phase I. A full oxidation of P correponds to $\Delta I/I = 3.5\times10^{-3}$.

All the experiments presented in the following were performed using benzoquinone-treated cells, i.e., in conditions in which a significant fraction of the ubiquinone pool is oxidized, in order to minimize the contribution of the back reactions in the reduction of P^+.

3.2. Kinetics of phase II as a function of temperature

The experiments in Figs. 4 and 5 were performed in the presence of 20 μM myxothiazol, which fully blocks phase III [10]. Such a high myxothiazol concentration is required to fully inhibit the Q_O-site, due to the high cell concentration we use in the 0.2-mm thick cuvette. In these conditions, membrane potential increases can be ascribed exclusively to phases I and II. We observed that repetitive-flash illumination given at temperature below 0°C in the presence of myxothiazol induces a progressive reduction of the ubiquinol pool. This is very likely due to the inhibition by myxothiazol of the process of ubiquinol oxidation. Consequently, the number of actinic flashes given in the presence of myxothiazol at temperatures below 0°C was limited to 30, in order to avoid a too large reduction of the ubiquinol pool. At 20°C (not shown), phase II is roughly monophasic and completed in ≈ 500 μs. At -7°C in the liquid state (Fig. 4), the kinetics of phase II is slowed down and displays two phases. A first phase (phase IIa) is completed in ≈ 1 ms and its amplitude is $\approx 9\%$ of phase I. The second phase (phase IIb) is completed in ≈ 10 ms with an amplitude of $\approx 15\%$ of phase I. Freezing the sample at -7°C does not modify the amplitudes of phases IIa and IIb but slows down phase IIb by a factor of about 2 (note the different time-scales). Lowering the temperature below -7°C leads to a progressive and parallel decrease of the amplitudes of phases IIa and IIb. At -20°C, phase II is fully inhibited.

In Fig. 5, we compare the kinetics of phase II and P^+ reduction in the liquid or the frozen state, at the same temperature (-7°C). The reduction of P^+ displays two phases. A first phase is completed in 10 ms in liquid state. The slower phase, ($t_{1/2} \approx 5$ s, in the liquid state) corresponds to a fraction ($\approx 25\%$) of the RCs not connected to the secondary donors. This fraction varies between 10% and 30% depending upon the bacterial culture. Freezing the sample increases the extent of P oxidation measured 50 μs after the flash and slows down the kinetics of P^+ reduction of about a factor 2. Comparison of the kinetics of phase IIb and that of the fast phase of P^+ reduction shows that these processes well correlate, both in the liquid and the frozen states. The half-times of these processes are ≈ 1.25 ms and ≈ 3.5 ms in the liquid and the frozen states, respectively. We have measured under similar conditions the kinetics of cyt c_t oxidation (not shown): cyt c_t oxidation correlates with the fast phase of P^+ reduction, but not with the slower phase. Moreover, as will be discussed in detail later (Fig. 10), a decrease in the amplitude of the μs phase in the cyt c_t oxidation is associated with the increase of the extent of oxidized P^+ in the same time-range, when the sample is frozen.

Fig. 6 shows the kinetics of phase II measured at -8°C, in the liquid and the frozen states, with a better time resolution than in Figs. 4 and 5. The experiment was performed in the absence of myxothiazol in order to prevent the progressive reduction of the ubiquinone pool. The fast increasing phase corresponds to phase IIa and its amplitude is $\approx 9\%$ of phase I. The half-time (≈ 220 μs) is about equal in the liquid and the frozen state. On the other hand, the second phase, mainly associated with phase IIb, is slowed down by about a factor 2, as already shown in Fig. 5.

3.3. Kinetics of phase III as a function of temperature

The experiments of Figs. 7 and 8 were performed in the absence of myxothiazol and in the presence of KCN. The sample was incubated at 16°C in the measuring cuvette, and the kinetics of the slow electrogenic rise (phase II + phase III) was followed along a series of saturating flashes given 1 min apart. During a 20 min-incubation period, the half-time of (phase II + phase III) progressively decreased from 7 ms to a minimum and steady-state value of 2.5 ms. This acceleration of phase III is associated with a partial reduction of the ubiquinone pool. According to Crofts et al. [15], the maximum rate of phase III (or the maximum rate of ubiquinol oxidation at site Q_O) is reached when at least 10% of the ubiquinone pool is reduced. After the incubation period, the kinetics of the membrane potential increase were measured at temperatures between 16°C and −22°C.

Fig. 7 shows the initial phases of the membrane potential increase measured at −18°C. The increasing phase ($t_{1/2} \approx 800$ μs) can be ascribed to phase IIa. Its amplitude is ≈9.5% of phase I, i.e., very similar to that measured in the experiments of Figs. 3, 5 and 6. Contrary to what we observed in the presence of myxothiazol (Fig. 4), the amplitude of phase IIa remained independent of the temperature between −10°C and −18°C (not shown). Both phases

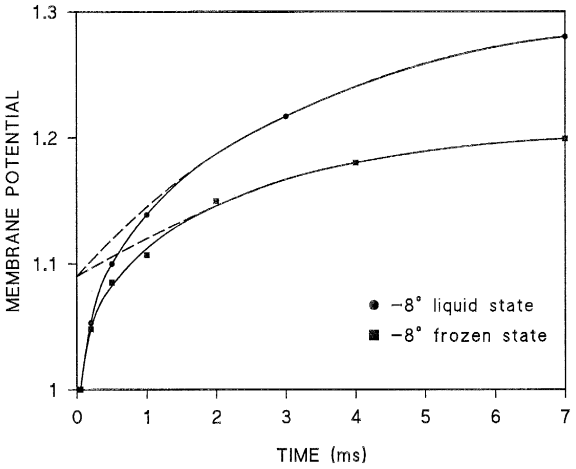

Fig. 6. Kinetics of phase IIa at −8°C in the liquid or the frozen state. Benzoquinone-treated cells. 0.25 mM KCN. 10 min incubation at room temperature. Saturating-flash excitation 1 min apart. The membrane potential is normalized to the amplitude of phase I.

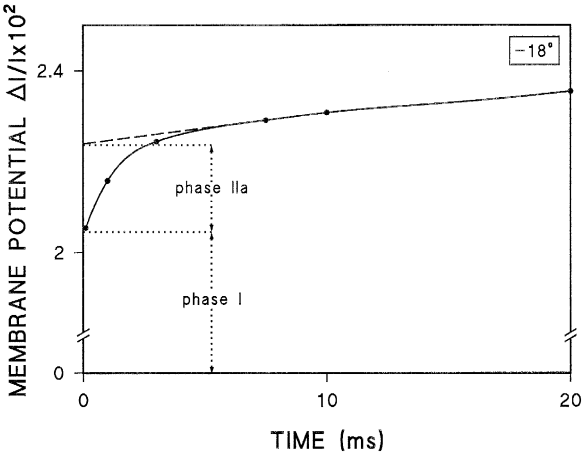

Fig. 7. Kinetics of phase IIa at −18°C. Benzoquinone-treated cells. 2 mM KCN. 15 min incubation at 16°C. Saturating-flash excitation 2 min apart.

IIb and III contribute to the slow rise following phase IIa.

Fig. 8 displays the kinetics of (phase IIb + phase III) computed by subtracting (phase I + phase IIa) from the membrane potential rise at temperatures between −10°C and −22°C. Between −22°C and −10°C, (phase I + phase IIa) was measured as shown in Fig. 7. At temperatures above −6°C, phase IIa cannot be accurately separated from phase IIb and we assumed that its amplitude was the same as at lower temperature. The amplitude of (phase IIb + phase III) remains fairly constant between 16°C and −14°C and close to 1. Freezing the sample induces no change in the amplitude of phase III, which implies that the number of charges transferred from the RCs to the cyt b/c_1 complexes is not modified. Using the same protocol as in Fig. 5, we measured the kinetics of reduction of P^+ and conclude that, in this batch, 15% of the RCs are not connected to the secondary donors.

Fig. 9 shows the logarithm of the rate of the membrane potential increase associated with (phase IIb + phase III), computed from Fig. 8, and plotted as a function of the reciprocal of the absolute temperature (Arrhenius plot). At each temperature the rate has been measured at an ordinate of 0.2 arbitrarily chosen, as phase IIb cannot be kinetically separated from phase III. The activation enthalpy does not markedly change during the course of the kinetics showing that phase IIb and phase III are limited by

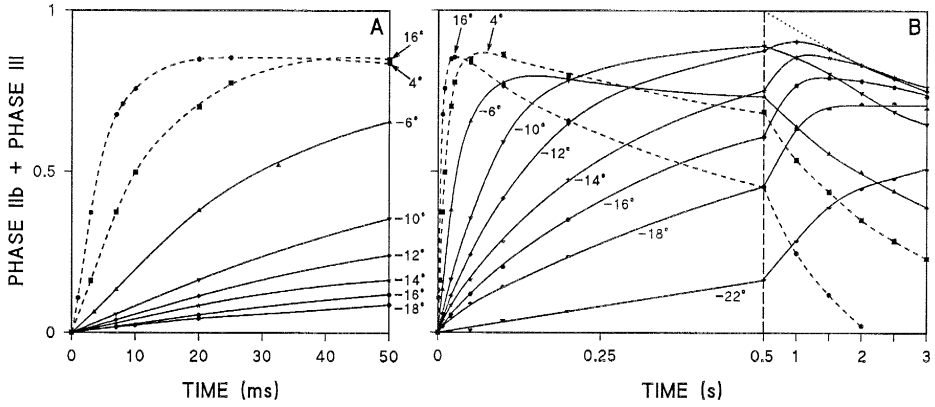

Fig. 8. Kinetics of (phase IIb + phase III) as a function of temperature. Same sample as in the experiment in Fig. 7. Saturating-flash excitation 1 min apart in the liquid state and 2 min apart in the frozen state. The amplitude of (phase IIb + phase III) is normalized to the amplitude of (phase I + phase IIa). From the kinetics of P^+ reduction (not shown), we estimated the fraction of RCs not connected to secondary donors to ≈ 15%.

the same process. One can separate two linear domains corresponding to the liquid and the frozen states. The activation enthalpy of (phase IIb + phase III) is 50 kJ mol^{-1} in the liquid state and 135 kJ mol^{-1} in the frozen state (between −10°C and −16°C).

Fig. 10 shows the time-resolved spectra following a saturating flash given at −8°C (the liquid state) or −12°C (the frozen state). In the liquid state, the maximum amount of photooxidized cyt c_t (551 nm trough) is close to that observed in the presence of myxothiazol (not shown). This oxidation phase is associated with the reduction of P^+ (decrease at 542 nm). About the half of cyt c_t is oxidized 50 μs after the flash. This μs-oxidation phase of cyt c_t is associated with the fraction of RCs possessing a bound cyt c_2. In the frozen state, the maximum amount of photooxidized cyt c_t is 2.5 times lower than that measured in the liquid state. As already reported in Fig. 8, we have checked that, in this batch, this decrease in the amount of oxidized cyt c_t is not associated with a decrease in the amplitude of phase III. In frozen state, there is no more oxidized cyt c_2 50 μs after the flash. This shows that freezing the suspension decreases the affinity of cyt c_2 for the RCs.

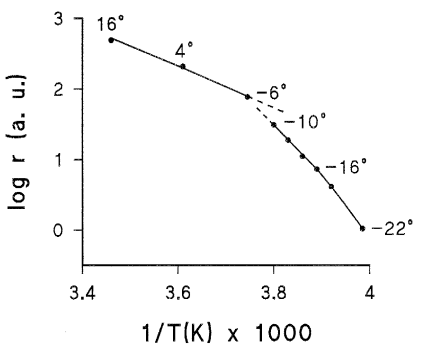

Fig. 9. Temperature-dependence of the rate r of phase III (Arrhenius plot). Data from Fig. 8. The rate of (phase IIb + phase III), expressed in arbitrary units, is measured at an ordinate of 0.2 (see text).

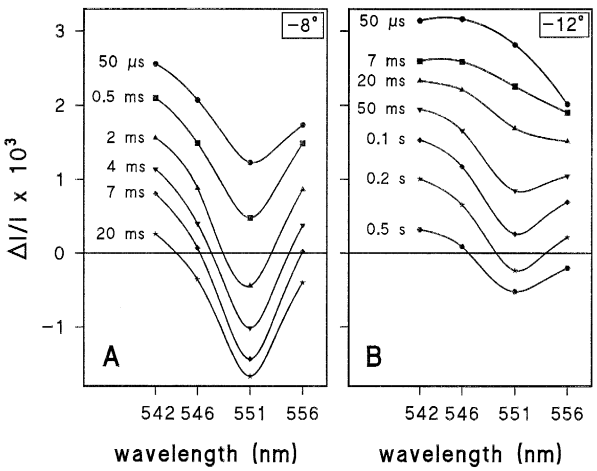

Fig. 10. Time-resolved flash-induced spectra at −8°C (the liquid state) or −12°C (the frozen state). Benzoquinone-treated cells. 2 mM KCN. 15 min incubation at room temperature. Saturating-flash excitation 1 min apart in the liquid state and 2 min apart in the frozen state.

4. Discussion

4.1. Membrane potential decay

In the liquid state, the Arrhenius plot of the membrane potential decay (Fig. 1) is linear between 16°C and −6°C, which suggests that no lipid transition occurs in this temperature range. Freezing the sample in the presence of DMSO induced no drastic change in the permeability of the membrane. The higher activation enthalpy that we observed in the frozen state can be due either to a structural change of the lipid bilayer or to a change of the properties of water in direct contact with the membrane.

4.2. Back reactions

Experiments in Fig. 2 show that at −32°C and irrespective of the redox potential, the membrane potential decay is mainly due to back reactions between P^+ and the reduced quinone acceptors. In reducing conditions, the ubiquinone pool is reduced and all the RCs are in a $PQ_AQ_BH_2$ state. The back reaction involves the reduced form Q_A^- of the primary acceptor, according to reaction (A):

$$P^+Q_A^-Q_BH_2 \rightarrow PQ_AQ_BH_2 \quad (A)$$

The kinetics of reaction (A) is roughly monophasic with $t_{1/2} \approx 23$ ms, i.e., about 3 times shorter than that measured at room temperature in isolated RCs (75 ms [16]). This suggests that the rate of reaction (A) differs in whole cells and in isolated RCs. In more oxidizing conditions, most of the membrane potential decay and of P^+ reduction occurs with a half-time of ≈ 3 s. We assume that most of the RCs have their secondary acceptors in the Q_B state. For this fraction of the RCs, the back reaction will involve the Q_B^- state of the secondary quinone acceptor, according to reaction (B).

$$P^+Q_AQ_B^- \rightarrow PQ_AQ_B \quad (B)$$

The half-time of back reaction (B) is ≈ 3 s, i.e., about 3 times slower than that measured at room temperature [16]. The fast phase of small amplitude which is completed in a time-range close to that measured in reducing conditions (≈ 200 ms) is very likely associated with a fraction of the RCs (≈ 30%) having their secondary quinone acceptor blocked in the Q_BH_2 state and back-reacting according to reaction (A).

4.3. Phase II

The results shown in Figs. 3–5 confirm that two independent processes are at the origin of phase II [8,9]. Phase IIa, completed in about 2 ms at −12°C is a much faster process than the oxidation of cyt c_t measured at the same temperature (see spectra Fig. 10). If we assume, as proposed in Refs. [8,9], that phase IIa is associated with the protonation of the doubly reduced acceptor $Q_B^=$, we expect that under repetitive-flash excitation, only half of the RCs includes a secondary acceptor in the Q_B^- state and will give rise to phase IIb. Thus, the electrogenicity associated with the transfer of 2 protons to $Q_B^=$ is 18% of that corresponding to the electron transfer from P to Q_A (phase I), i.e., 9% per proton transferred. As shown in Fig. 6, freezing the sample does not modify the rate of protonation, which is an intracomplex process.

Phase IIb is associated with the reduction of P^+ (Fig. 5), as previously proposed in [5,6]. In the frozen state, ≈ 0.67 P^+ is reduced between 50 μs and 20 ms. In the same time-range, the amplitude of phase IIb is ≈ 0.15 of phase I. Therefore, the electron transfer from cyt c_2 to P^+ induces an electrogenic phase of 0.15/0.67 ≈ 0.22 of that associated with the electron transfer from P to Q_A. We conclude that the electrogenicity associated with the transfer of one electron from P to Q_A is $1-0.22-0.09=0.69$ of that corresponding to the transfer of one electron from one side to the other side of the membrane. In contrast with phase IIa, the rate of P^+ reduction and phase IIb are slowed down by a factor of about 2 in the frozen state. The activation enthalpy of phase IIb in the frozen state is close to that we have measured for cyt c_t oxidation (≈ 120 kJ mol^{-1}, not shown), while that of phase IIa, computed between −8°C and −18°C is ≈ 70 kJ mol^{-1}.

In the frozen state (Fig. 4), the amplitudes of phases IIa and IIb vary in a similar way when the temperature is lowered from −7°C to −20°C. This correlation can be understood if phase IIa is exclusively associated with the protonation of $Q_B^=$, as proposed in Refs. [8,9]. In oxidizing conditions and at temperatures above −18°C, electron transfer from

cyt c_2 to P^+ is faster than the back reactions between P^+ and the reduced quinone acceptors. Then, half of the RCs includes secondary acceptors in the Q_B^- state and in these RCs, flash excitation induces the formation of $Q_B^=$. We then predict that phase IIa and phase IIb have a maximum extent (see Fig. 7). When the ubiquinone pool is partially reduced, the back reactions are accelerated, due to the occurrence of back reaction (A), which then compete more efficiently with the reduction of P^+ by cyt c_2 than in oxidizing conditions. This is shown in Fig. 4, in which repetitive-flash excitation in the presence of myxothiazol induces a reduction of the ubiquinone pool. In these conditions, a decrease in the amplitude of both phase IIa and phase IIb is already observed at -12°C.

4.4. Phase III

At -12°C in the frozen state, the amplitude of the sum (phase IIb + phase III) is about equal to that of (phase I + phase IIb) (see dotted line, Fig. 8). If one assumes that phase IIb is about 13% of (phase I + phase IIb) (see Fig. 4), the amplitude of phase III divided by the sum of the amplitudes of (phase I + phase IIa + phase IIb) is ≈ 0.77. For the RCs connected to the secondary donors ($\approx 85\%$ in this batch), the amplitude of phase III is close to that of (phase I + phase II). Thus, the amplitude of phase III corresponds to the transfer of about one charge across the membrane per photoreaction, i.e., the maximum yield of the electrogenic phase associated with the Q-cycle process [15,17]. We then conclude that, at temperatures above -16°C, all the positive charges formed at the level of the primary donor are transferred to the cyt b/c_1 complex as well in the liquid as in the frozen state. Below -16°C, the rate constant of cyt c_t oxidation becomes close to the rate constant of back reaction (B) ($t_{1/2} \approx 3$ s). Then, these two processes compete for the reduction of P^+, leading to a decrease in the number of positive charges transferred to the cyt b/c_1 complex. Therefore, the decrease in the amplitude of (phase IIb + phase III) observed below -16°C does not imply a blockage of the lateral transfer of cyt c_2 between the two membrane complexes.

Irrespective of the structural organization of the photosynthetic electron transfer chain, the stoichiometry of 2 RCs/1 cyt c_2/1 cyt b/c_1 implies that, after a saturating flash, phase III involves the following sequence of 14 steps (Scheme 1).

(1) and (8) $P^+ + C_2 \rightarrow P^+C_2$
(2) and (9) $P^+C_2 \rightarrow PC_2^+$
(3) and (10) $PC_2^+ \rightarrow P + C_2^+$
(4) and (11) $C_2^+ + C_1FeS \rightarrow C_2^+C_1FeS$
(5) and (12) $C_2^+C_1FeS \rightarrow C_2C_1FeS^+$
(6) and (13) $C_2C_1FeS^+ \rightarrow C_2 + C_1FeS^+$
(7) and (14) $C_1FeS^+ + UQH_2 \rightarrow C_1FeS + UQ^- + 2\,H^+$

Scheme 1. C_2, cyt c_2; C_1FeS, high-potential chain of the cyt b/c_1 complex; UQH_2, ubiquinol.

In the liquid state, most of cyt c_2 bind to the RCs prior to flash excitation and the process starts mostly at step (2). In the frozen state, the affinity of cyt c_2 for the RCs is largely decreased (Fig. 8) and the process starts at step (1). In these conditions, 4 steps (1, 4, 8, 11) imply lateral movements of oxidized or reduced cyt c_2 between the two membrane complexes. If cyt c_2 were a diffusing species, we would expect that freezing the sample makes steps (1), (4), (8) and (11) rate-limiting. Then, the kinetics of phase III would depend upon several sequential second-order processes. On the other hand, if one assumes that the electron transfer chain is organized in supercomplexes, the lateral displacement of a single cyt c_2 molecule is restricted to a small domain including the binding sites of cyt c_2 to the RCs and to the cyt b/c_1 complex and then, all the steps in Scheme 1 would be first-order processes except steps (7) and (14).

At -8°C, in the liquid state (Fig. 10), the amount of oxidized cyt c_t is close to that measured in the presence of a saturating concentration of myxothiazol. This implies that cyt c_t oxidation, which involves steps (2) to (4) and (8) to (11), is a faster process than its reduction (steps (7) and (14)). In agreement with this conclusion, the half-time for P^+ reduction is about 20 times shorter than that of phase III. Thus, the activation enthalpy for phase III (50 kJ mol^{-1}, Fig. 9), determined in the liquid state, can be ascribed to the Q-cycle process. According to Crofts and Wang [18], the activation enthalpy for the process of cyt b reduction at the Q_O-site, measured in the liquid state, is 32 kJ mol^{-1}. The higher activation enthalpy we have measured for phase III suggests that, in the conditions of our experiments, the limit-

ing step in the Q-cycle process could be the reduction of quinone at site Q_I.

In the frozen state, the activation enthalpy measured between -10°C and -16°C is about 135 kJ mol^{-1}, i.e., close to the activation enthalpy we have measured for cyt c_t oxidation (120 kJ mol^{-1}). The amplitude of the transient oxidation of cyt c_t is about 3 times lower than in the liquid state. This implies similar rate constants for cyt c_2 oxidation and reduction. We then conclude that, in the frozen state, the overall rate of electron transfer processes is limited mainly by the rate of reduction of P^+ by cyt c_2 (steps (1) and (8)) and partly by the rate of quinol oxidation (steps (7) and (14)). This explains why the activation enthalpy for cyt c_t oxidation is close to that of phase III.

The analysis of phase III strengthens the conclusions that the photosynthetic electron transfer chain within the chromatophore membranes of *Rb. sphaeroides* is organized in supercomplexes. In the frozen sample, the overall rate of electron transfer appears as limited by the rate of cyt c_2 oxidation and by the rate of quinol oxidation at site Q_O. Neither the lateral movements of cyt c_2 between the two membrane complexes, nor the binding of cyt c_2 to the cyt b/c_1 complexes are rate-limiting. In the structural model we propose (Fig. 11A), we assume that, in the frozen state, a thin layer of water, located between the membrane and the ice surface, remains in the liquid state. The thickness of this layer must be close to the diameter of a cyt c_2 molecule (≈ 20 nm). Cyt c_2 is trapped in a pocket located between the two RCs and the cyt b/c_1 complex which form a supercomplex. In the frozen state, the overall rate of electron transfer in the photosynthetic chain is mainly limited by the rate of binding of cyt c_2 to the RCs rather than to the cyt b/c_1 complex. This suggests that cyt c_2 bound to the cyt b/c_1 complex does not protrude out of the membrane. An alternate hypothesis is that different binding sites of cyt c_2 to the RCs are involved in the liquid and the frozen states. In the frozen state, the binding site would be on the edge of the RC (Fig. 11B) with a longer distance between cyt c_2 and P than in the liquid state. Evidence for two cyt c binding sites to the RC, with different affinities, was proposed by Overfield and Wraight [19] and Drepper and Mathis (personal communication). Then, in the frozen state, the limiting step could be the intracomplex electron transfer. The presence of ice in the vicinity of the membrane perturbs the binding of cyt c_2 to the RCs but not the lateral movement of cyt c_2 between the two membrane complexes.

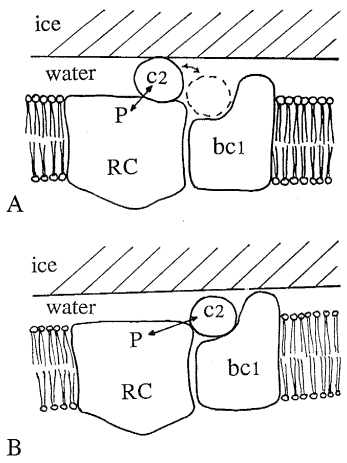

Fig. 11. Tentative structural models of the organization of the electron transfer chain in the frozen state. In these lateral views, only one reaction center of the supercomplex is represented.

It is interesting to comment on the large difference between the kinetics of phase III at -14°C (Fig. 3, $t_{1/2} \approx 1.6$ s) and in Fig. 8 ($t_{1/2} \approx 200$ ms). In the experiment Fig. 8, all the Q_O-sites include a ubiquinol molecule, which leads to a maximum rate of phase III. On the other hand, in the highly oxidizing conditions used in Fig. 3, the pool of ubiquinol is fully oxidized prior to the flash excitation. Following the flash, only the ubiquinol molecules formed at the level of the RCs are available at site Q_O. If ubiquinone is a diffusing species [20], the concentration of delocalized ubiquinol is not sufficient to saturate the Q_O-site, which leads to a slower phase III [15]. This implies that at -14°C, the mobile link established by quinol between the Q_B-site of the RCs and the Q_O-site of the cyt b/c_1 complex is still operative. Therefore, the lipid phase of the membrane should be fluid enough to allow quinone heads to move in directions parallel and perpendicular to the plane of the membrane. Because ubiquinone still diffuses and cyt c_2 still establishes a link between the RCs and the cyt b/c_1 within a supercomplex, the cyclic photosynthetic electron transfer chain remains operative at temperature below -14°C in *Rb. sphaeroides*.

Acknowledgements

The authors are indebted to J. Lavergne for his critical reading of the manuscript and helpful discussions. Thanks are also due to F. Drepper for valuable suggestions. This work has been supported partly by EEC contract BIO2-CT93-0076 (P.J., A.J.).

References

[1] Joliot, P., Verméglio, A. and Joliot, A. (1989) Biochim. Biophys. Acta 975, 336–345.
[2] Joliot, P., Verméglio, A. and Joliot, A. (1990) Biochemistry 29, 4355–4361.
[3] Verméglio, A., Joliot, P. and Joliot, A. (1993) Biochim. Biophys. Acta 1183, 352–360
[4] Joliot, P., Verméglio, A. and Joliot, A. (1996) Photosynth. Res. 48, 291–299.
[5] Jackson, J.B. and Dutton, P.L. (1973) Biochim. Biophys. Acta 325, 102–113.
[6] Dutton, P.L., Petty, K.M., Bonner, H.S. and Morse, S.D. (1975) Biochim. Biophys. Acta 387, 536–556.
[7] Wraight, C.A., Codgell, R.J. and Chance, B. (1978) In The Photosynthetic Bacteria (Clayton, R.K. and Sistrom, W.R., eds.), pp. 471–512, Plenum Press, New York.
[8] Kaminskaya, O.P., Drachev, L.A., Konstantinov, A.A., Semenov, A.Y. and Skulachev, V.P. (1986) FEBS Lett. 202, 224–228.
[9] Drachev, L.A., Mamedov, A., Mulkidjanian, A.Y., Semenov, A.Y., Shinkarev, V.P. and Verkhovsky, M.J. (1988) FEBS Lett. 233, 315–318.
[10] Meinhardt, S.W. and Crofts, A.R. (1982) FEBS Lett. 149, 217–222.
[11] Vredenberg, W.J. and Duysens, L.N.M. (1964) Biochim. Biophys. Acta 79, 456–463.
[12] Diner, B.A. and Joliot, P. (1976) Biochim. Biophys. Acta 423, 479–498.
[13] Joliot, P., Béal, B. and Frilley, B. (1980) J. Chim. Phys. 77, 209–216.
[14] Joliot, P. and Joliot, A. (1984) Biochim. Biophys. Acta 765, 210–218.
[15] Crofts, A.R., Meinhardt, S.W., Jones, K.R. and Snozzi, M. (1983) Biochim. Biophys. Acta 723, 202–218.
[16] Clayton, R.K. and Yau, H.F. (1972) Biophys. J. 12, 867–881.
[17] Mitchell, P. (1975) FEBS Lett. 57, 137–139.
[18] Crofts, A.R. and Wang, Z. (1989) Photosynth. Res. 22, 69–87.
[19] Overfield, R.E. and Wraight, C.A. (1986) Photosynth. Res. 9, 167–179.
[20] Venturoli, G., Fernandez-Velasco, J., Crofts, A.R. and Melandri, B.A. (1988) Biochim. Biophys. Acta 935, 258–272.